JOURNAL OF PROPULSION AND POWER
Vol. 33, No. 4, July–August 2017

Effects of Flow Compressibility and Density Ratio on Film Cooling Performance

Wenwu Zhou,* Blake Johnson,† and Hui Hu‡
Iowa State University, Ames, Iowa 50011

DOI: 10.2514/1.B36275

An experimental investigation was performed to examine the effects of flow compressibility and density ratio of coolant to mainstream flows on the performance of film cooling injected from a row of cylindrical holes over a flat plate. The experimental study was conducted in a transonic wind tunnel. A pressure-sensitive paint technique was used to map the corresponding adiabatic film cooling effectiveness distributions over the surface of interest, based on a mass flux analog to traditional temperature-based cooling effectiveness measurements. It was found that, at the relatively low blowing ratio of $M \leq 0.40$, the flow compressibility had almost no effects on the film cooling effectiveness over the surface of interest. At relatively high blowing ratios of $M \geq 0.85$, the film cooling effectiveness for the test case with compressible, transonic mainstream flow was found to become marginally better than that with the mainstream being incompressible. Although the density ratio was found to have limited effects on the film cooling performance at relatively low blowing ratios, it was found to affect the film cooling effectiveness substantially at relatively high blowing ratios. A denser coolant flow would result in a better film cooling protection to the surface of interest.

Nomenclature

D	=	diameter of coolant injection hole
DR	=	coolant to mainstream density ratio; ρ_c/ρ_∞
I	=	coolant to mainstream momentum ratio; $\rho_c U_c^2/\rho_\infty U_\infty^2$
Le	=	Lewis number; α/D_s
M	=	blowing ratio or mass flux ratio; $\rho_c U_c/\rho_\infty U_\infty$
Ma	=	Mach number
Ma_c	=	convective Mach number
$(p_{o_2})_{air}$	=	partial pressure of oxygen with air as the coolant
$(p_{o_2})_{mix}$	=	partial pressure of oxygen with nonoxygen gas as the coolant
T_{aw}	=	adiabatic wall temperature
T_r	=	mainstream recovery temperature
T_{tc}	=	stagnation temperature of coolant
U_c	=	coolant stream velocity
U_∞	=	incoming flow velocity
η	=	film cooling effectiveness
$\overline{\eta}_{area\text{-}averaged}$	=	area-averaged film cooling effectiveness
θ_0	=	total temperature ratio of coolant to mainstream

I. Introduction

IN SEARCH of the higher thermal efficiency and power output of gas turbine engines, the turbine inlet temperature is continuously being pushed upward, causing the proper protection of hot section components from extremely high temperatures to be of critical importance. Film cooling technology has been developed out of the necessity to protect turbine hot section components from damage mechanisms, such as corrosion and melting, despite the severe temperatures in which they operate. By releasing a film of coolant gas on the component surfaces, the turbine elements can be isolated from the hot gasses, hence increasing their lifetime. There is an inherent desire to optimize the film cooling systems to further increase the efficiency of gas turbines, which can result in significant economic savings. However, a better understanding of the underlying physics pertinent to film cooling is essential for such optimization.

Extensive experimental studies have been conducted in recent years on film cooling for improved cooling effectiveness. For example, Goldstein et al. [1] reported a remarkable enhancement of film cooling effectiveness by using fan-shaped holes, which employed a diffuser to reduce the momentum of the coolant jet at the hole exit. Baldauf et al. [2,3] studied the influence of the mass flux ratio, density ratio, and other relevant factors on film cooling effectiveness over a flat surface by using an infrared thermal imaging technique. Bogard and Thole [4,5] and Bunker [6] provided comprehensive reviews on film cooling studies, and they summarized that empirical correlations would be failing in characterizing the curvature effects, hole shape effects, and other effects on film cooling effectiveness of circular coolant injection holes.

It should be noted that, although the hot gasses passing through stages of turbine blades are usually compressible, transonic flows, most of the previous studies on film cooling were conducted with the mainstream and coolant stream being low-speed incompressible flows (i.e., the Mach number of the flows being smaller than 0.2). Only a few studies can be found in the literature to examine the effects of flow compressibility on the performance of film cooling. Gritsch et al. [7], who measured the cooling effectiveness of a single coolant hole over a range of Mach numbers (i.e., $Ma = 0.3$, 0.60, and 1.2), found that the measured effectiveness had little dependence on the Mach number of the flow. Liess [8] performed a similar study, but with a positive pressure gradient along the test plate, and confirmed the limit effects of flow compressibility on the film cooling performance. Repukhov [9] also found that the compressibility effects on film cooling performance were very small over a wide range of test conditions. On the contrary, Dellimore et al. [10] and Parthasarathy and Zakkay [11] investigated the compressibility effects on film cooling effectiveness, and they concluded that compressibility effects could be significant once the Mach numbers of the flows were high enough. Although those previous studies uncovered useful information, some of the inconsistencies noted raise concerns, and no consensus has been reached yet regarding the effects of flow compressibility on film cooling performance. Therefore, it is highly desirable to examine the effects of flow compressibility on the film cooling performance more comprehensively in order to clarify the discrepancies. This is essential to improve our understanding of the underlying physics for the optimal

Received 28 March 2016; revision received 27 September 2016; accepted for publication 5 October 2016; published online 28 December 2016.

*Postdoctoral Associate, Department of Aerospace Engineering.
†Postdoctoral Associate, Department of Aerospace Engineering; currently Department of Mechanical Science and Engineering, University of Illinois at Urbana–Champaign, Champaign, IL 61801.
‡Professor of Aerospace Engineering, Department of Aerospace Engineering; huhui@iastate.edu. Associate Fellow AIAA (Corresponding Author).

film cooling design to provide a better protection to the hot components of gas turbine engines.

It should also be mentioned that, due to the limited temperature differences between the coolant and mainstream flows used in most of the previous heat transfer studies on film cooling [2,12–14], the experimental investigations were performed with the density ratio ($DR = \rho_c/\rho_\infty$) being very small: approximately 1.0. However, in real gas turbine engines, the density ratio of the coolant to the mainstream flow would be usually in the range of $1.5 \sim 2.0$ [15,16], caused by the significant temperature differences between the streams. Hansmann et al. [17] studied the tangential-slot film cooling of a flat plate in a high-enthalpy wind tunnel ($0.5 < Ma < 1.0$), and they found that the measured cooling effectiveness strongly depended on the density ratios, with heavier coolant gas leading to enhanced film cooling effectiveness. Pedersen et al. [18] conducted a similar study, but with low-speed incompressible flow as the mainstream flow, and they found that the effectiveness of film cooling would increase greatly as the density ratio increased, especially at large blowing ratios ($M > 1$). Maqbool et al. [19] measured the film cooling performance of a tangential slot under supersonic flow conditions with varied density ratios of the coolant to mainstream flows. Meanwhile, pertinent to the entrainment and mixing process of turbulent shear flow in film cooling, Urban and Mungal [20], Hall [21], Rossmann et al. [22], and Rossmann [23] examined the compressibility effects on the growth rate of turbulent mixing shear layers and the development of large-scale structures in high-Mach-number flows with various density ratios of the two streams. However, the effects of the density ratio between the coolant and mainstream flows on the performances of film cooling over the protected surfaces have not been fully explored, especially for the test conditions with the mainstream and coolant being compressible, transonic flows.

In the present study, a comprehensive experimental investigation was performed to examine the effects of flow compressibility and density ratios of the coolant to mainstream flows on the film cooling performance at different blowing ratios (i.e., mass flux ratios). The experimental study was conducted in a transonic wind tunnel available at Iowa State University. During the experiments, coolant streams were injected from an array of circular holes at an inclined injection angle of $\alpha = 35$ deg with respect to the mainstream flow direction. Although the Mach numbers of the mainstream flow were set to be $Ma = 0.07$ (i.e., incompressible low-speed flow), 0.30, 0.50, and 0.70 (i.e., compressible, transonic flow), the tested blowing ratios (i.e., mass flux ratio, $M = \rho_c U_c/\rho_\infty U_\infty$) of the coolant injection were selected to be $M = 0.40$ (low), 0.85 (medium), and 1.25 (high), respectively. The density ratio of the coolant to mainstream flows (i.e., $DR = 1.0$, 1.5, and 2.0) was also varied during the experiments to evaluate its effects on the performance of film cooling at different blowing ratios. A pressure-sensitive paint (PSP) technique was used to map film cooling effectiveness distributions on the surface of interest, based on a mass flux analog to traditional temperature-based cooling effectiveness measurements. A high-resolution particle image velocimetry (PIV) system was also used to conduct flowfield measurements to correlate with the adiabatic film cooling effectiveness measurements. It is worth mentioning that some of the preliminary results of this effort were presented in our recent conference paper [24]. The present work adds much more detailed measurement results, extensive discussions, and considerable analysis to elucidate the underlying physics, which is far beyond the scope of our conference paper [24].

II. Experimental Setup and Test Model

A. Wind-Tunnel Facility and Test Model

The present experimental study is conducted in a transonic open-circuit wind tunnel located at the Department of Aerospace Engineering of Iowa State University. As shown schematically in Fig. 1, the transonic wind tunnel has an optically transparent test section with 63.5×25.4 mm in cross section. The transonic airflow is supplied by using three big pressurized tanks, which are about 8.0 m^3 in volume and 150 psi in pressure at full capacity. A ceramic flow straightener with square 1.0 mm^2 cells is installed upstream of the contraction to create a uniform low-turbulence incoming flow upstream of the test section. Six pressure taps and two K-type thermocouples are placed along the test rig to acquire instantaneous temperature and pressure data inside the test section and plenum. With all three tanks fully pressurized, the mainstream flow inside the test section can be maintained as a transonic flow (i.e., $Ma = 0.70$) for about 5.0 min, with the flow velocity variation within $\pm 2.0\%$. For each test, experimental data are acquired within a duration time of less than 180 s, after a transient period of 30 s at the beginning. The temperature drop in the incoming flow at the entrance of the test section is found to be less than 3°C during each test run.

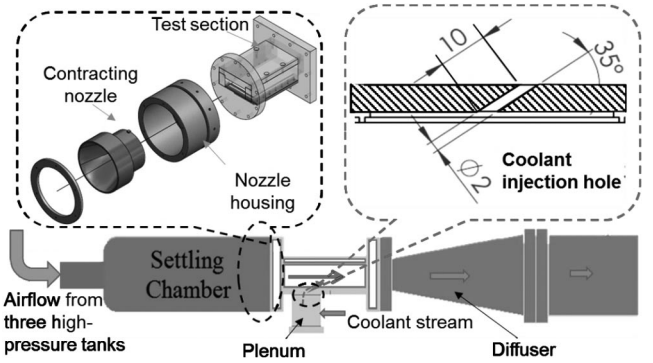

Fig. 1 Schematic of the transonic wind tunnel used for the present study.

The test plate is made of a rigid, hard plastic material by using a rapid prototyping additive manufacturing printer. The upper surface of the test plate is polished carefully with fine sandpapers and special plastic polishes to achieve a very smooth, glossy finish. A row of five circular holes with a diameter of $D = 2.0$ mm and an inclined injection angle of $\alpha = 35$ deg are designed to inject coolant streams into the mainstream flow as cross jet flows. The spanwise pitch between the adjacent coolant injection holes is designed as $3D$, and the entry length of the cooling holes is $5D$. The test model is mounted on a plenum chamber and sealed by a thin latex runner gasket and silicon, as shown schematically in Fig. 1.

In the present study, although the transonic airflow from the three pressurized tanks was used to represent the hot mainstream gas in a typical gas turbine stage, an oxygen-free gas was used to simulate the coolant streams injected from the circular coolant injection holes. In the present study, the Mach number of the mainstream flow was held at four preset levels, i.e., $Ma = 0.07$ (baseline case), 0.30, 0.50, and 0.70, respectively. A stripe tape of 1.0 mm in thickness was applied at the leading edge of the test section (i.e., $28D$ upstream of coolant injection hole) to trip the mainstream flow to ensure a fully developed turbulent boundary layer over the test plate. The boundary-layer thicknesses of the mainstream flow at the upstream of the coolant injection holes, which were measured by using a PIV system, were found to be $\delta_{99} \approx 0.7 \sim 1.2D$, with the Mach number of the mainstream flow changing from $Ma = 0.70$ (i.e., compressible, transonic flow case) to $Ma = 0.07$ (baseline case); the corresponding momentum thicknesses and the shape factors were found to be $0.06D \sim 0.09D$ and $1.4 \sim 1.5$, respectively. Additionally, the corresponding Reynolds number level ($\rho U_\infty l/\mu$, where l is the distance from the leading edge to the coolant injection hole) was found to vary from 88,000 to 836,000, corresponding to the low-speed baseline case ($Ma = 0.07$) and the transonic flow case ($Ma = 0.70$).

The oxygen-free coolant gas from a pressurized gas cylinder would pass through a long pipeline and a constant temperature thermal bath before finally entering into the plenum chamber. All the experiments were conducted at an isothermal condition, with the environmental temperature being $T = 22 \pm 0.5$°C. To simulate the scenarios with different density ratios between the hot mainstream gas and coolant streams caused by the different temperatures between the two streams in a real gas turbine engine, Nitrogen (N_2), Carbon dioxide (CO_2), or a mixture of Sulfur hexafluoride (SF_6) and CO_2 was used in the present study as the coolant gas. As a result, the corresponding density ratio between the coolant and mainstreams was found to be $DR \approx 1.0$, 1.5, and 2.0, respectively. During the experiments, the corresponding

Table 1 A summary of the major flow parameters of the test cases

Ma	DR	M	Ma_{c1}	Ma_{c2}	θ_0
0.07	1.0	0.40, 0.85, 1.25	— —	— —	1.00
0.07	1.5	0.40, 0.85, 1.25	— —	— —	1.00
0.07	2.0	0.40, 0.85, 1.25	— —	— —	1.00
0.30	1.5	0.40, 0.85, 1.25	0.03-0.12	0.03 ~ 0.13	1.00
0.50	1.5	0.40, 0.85, 1.25	0.04-0.20	0.05 ~ 0.21	1.00
0.70	1.0	0.40, 0.85, 1.25	0.08-0.21	0.09 ~ 0.21	1.00
0.70	1.5	0.40, 0.85, 1.25	0.06-0.28	0.07 ~ 0.30	1.00
0.70	2.0	0.40, 0.85, 1.25	0.15-0.31	0.16 ~ 0.34	1.00

blowing ratio (i.e., mass flux ratios of $M = \rho_c U_c/\rho_\infty U_\infty$) were also monitored by using mass flow meters (Omega, FMA-1600A). Following up the work of Dellimore et al. [10], Dellimore [25], and Papamoschou and Roshko [26], the convective Mach numbers [$Ma_{c1} = (U_\infty - U_w)/a_\infty$, $Ma_{c2} = (U_c - U_w)/a_c$] and total temperature ratio of the coolant to the mainstream (i.e., $\theta_0 = (T_{0c}/T_{0\infty})$) were also calculated, where U_w was the moving velocity of dominant flow structures and could be obtained by the following equation [26]:

$$\left(1 + \frac{\gamma_1 - 1}{2} Ma_{c1}\right)^{(\gamma_1/(\gamma_1-1))} = \left(1 + \frac{\gamma_2 - 1}{2} Ma_{c2}\right)^{(\gamma_2/(\gamma_2-1))}$$

where a_∞ and a_c are the speeds of sound in the mainstream and coolant flows, respectively. The major controlling parameters for the test cases are listed in Table 1.

B. Adiabatic Film Cooling Effectiveness Measurement by Using PSP Technique

Traditionally, the adiabatic film cooling effectiveness η is defined in terms of recovery temperatures, which is expressed as

$$\eta = \frac{T_r - T_{\text{aw}}}{T_r - T_{\text{tc}}} \tag{1}$$

where T_r is the mainstream recovery temperature, T_{aw} is the adiabatic wall temperature of the surface under inspection, and T_{tc} the total temperature of the coolant flow at the exit of the coolant injection hole. Obviously, the primary challenge associated with the temperature-based methods is in measuring the true adiabatic wall temperature, despite the physical reality of heat conduction within the test model.

It should be noted that, because the Lewis number ($Le = \alpha/D_s$, where α is thermal diffusion coefficient and D_s is the concentration diffusion coefficient) is approximately 1.0 for airflow, the thermal boundary layer and concentration boundary layer are of the same order, allowing the differential equations involving heat and mass transfer to be analogous [27–29]. Based on a mass transfer analog to traditional thermal-based measurements, a pressure-sensitive paint technique has been widely used in recent years to measure adiabatic film cooling effectiveness distributions on the surfaces of interest [30–32]. Because PSP measurements are usually conducted by performing "cold" experiments at isothermal conditions, the concerns and implications due to effects of heat conduction through the test models on the adiabatic wall temperature measurements can be easily eliminated. As for the test cases with a transonic flow involved in the present study, the mass transfer analogy should still be valid because the effects of pressure P on the thermal diffusion coefficient

$$\alpha = \frac{\lambda}{\rho c_p} = \left(\frac{\lambda RT}{c_p}\right)\frac{1}{P}$$

and concentration coefficient

$$D_s = D_{s,\text{atm}}\left(\frac{T}{T_{20^\circ\text{C}}}\right)\frac{P_{\text{atm}}}{P}$$

will be cancelled out in calculating the Lewis number.

In PSP experiments, the surface of interest is coated with an oxygen-sensitive layer of paint, which consists of luminophores molecules held bound within a gas-permeable polymeric binder. When excited by certain UV light, the luminophores molecules would emit light. However, the excited molecules may return to ground state via a reduced or radiationless emission in the presence of oxygen molecules, which is called oxygen quenching [33]; and the intensity of the photoluminescence is inversely proportional to the concentration of local oxygen. Consequently, the concentration of oxygen over the interested surface can be calculated based on the recorded light intensity through the using of a calibration curve [32]. Applying the concentrations of oxygen rather than the temperature into Eq. (1), the adiabatic film cooling effectiveness can be expressed as Eq. (2), as described by Charbonnier et al. [34], where MW is the ratio of molecular weights of the coolant gas to the freestream gas:

$$\eta = 1 - \frac{1}{[((p_{\text{o}_2})_{\text{air}}/(p_{\text{o}_2})_{\text{mix}})_{\text{wall}} - 1]\text{MW} + 1} \tag{2}$$

The pressures in Eq. (2) can be determined based on the recorded intensity of the emission light, which is directly related to the partial pressure of oxygen. The mathematical function between the normalized intensity and partial pressure of oxygen can be obtained through a dedicated PSP calibration process. Further information about the technical basis of the PSP technique, image procedure, and calibration procedure for film cooling effectiveness measurements can be found in [27,30–32].

It should be noted that Johnson et al. [32] conducted a comparative study to compare the measured film cooling effectiveness data of their PSP measurements against those derived directly from the temperature-based measurements of Baldauf et al. [2] under the same or comparable test conditions. They found that the measured film cooling effectiveness data with the PSP technique agreed well with those derived directly from temperature-based measurements. By using similar experimental setups to those of Johnson et al. [32], a PSP technique was used in the present study to map the adiabatic film cooling effectiveness distribution over the test plate at different test conditions. Figure 2 shows the experimental setup used for the PSP measurements. A constant UV light [LM2X-DM, Innovative Science Solutions, Inc. (ISSI)] with a wavelength of 390 nm was used as the excitation source for the PSP measurements. A 14-bit (2048 × 2048 pixel) charge-coupled device camera (PCO2000, Cooke Corporation) with a 610 nm long-pass filter was used to record the photoluminescence light emitted by excited PSP molecules. The PSP used in the present study was UniFIB (provided by ISSI), which had a low sensitivity to temperature variation (~0.5%/°C). As mentioned previously, the variations of the freestream temperature during each test run were found to be less than 3°C, and the measurement uncertainty caused by the temperature changes of the freestream temperature would be less than 2.0%.

In the present study, interrogation windows of 9 × 9 pixels in size with a 50% overlap were used for the PSP image processing in order to minimize the effects of random noises in the acquired images on the PSP measurements. The acquired PSP images have a

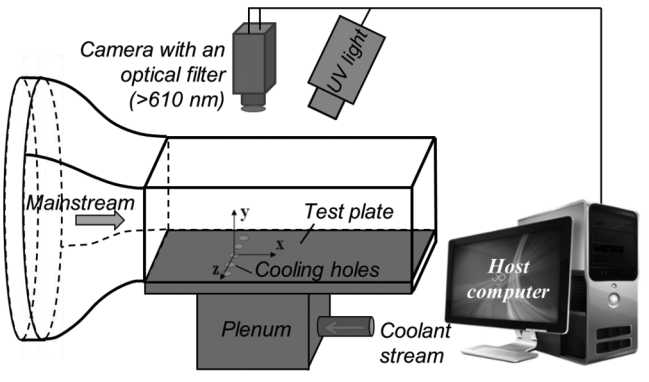

Fig. 2 Experimental Setup for the PSP measurements.

magnification of 0.055 mm/pixel, resulting in a spatial resolution of ~0.25 mm for the PSP measurements. The measurement uncertainty of the film cooling effectiveness, after taking the effects of temperature variations during each run into account, was estimated to about 5% for $\eta = 0.5$ and 10% for $\eta = 0.3$ (i.e., absolute uncertainty $\Delta\eta \approx 0.03$). Further information about the uncertainty analysis of the PSP measurements can be found in the work of Johnson and Hu [35].

C. Flowfield Measurements by Using PIV Technique

In addition to mapping film cooling effectiveness distributions based on PSP measurements, a high-resolution PIV system was also used in the present study to conduct detailed flowfield measurements to quantify the dynamic mixing process between the coolant and mainstream flows over the test plate. For the PIV measurements, both the coolant gas and mainstream flow were seeded with ~0.5 μm bis (2-ethylhexyl) sebacate oil droplets generated by using aerosol generators (TSI, model 9306). Based on the work of Melling [36], the tiny seeding droplets for PIV measurements would be able to reach 99% of the freestream velocity in less than 0.60 μs, which was much smaller than the time scales involved in the present study. A neodymium-doped yttrium aluminium garnet (Nd:YAG) laser (New Wave Gemini PIV 200) was used to emit two pulses of 200 mJ laser light at a 532 nm wavelength with a repetition rate of 5 Hz. A set of high-energy mirrors and optical lenses were used to shape the laser beam into a thin light sheet of 0.5 mm in thickness in the measurement window. To reveal the interaction between the coolant stream and the mainstream flow, the illuminating laser sheet was aligned along the flow direction of the mainstream, bisecting the circular coolant hole in the middle of the test plate. A high-resolution digital camera (14-bit, 2048 by 2048 pixels, PCO2000) was used for the PIV image acquisition with a field of view of 7.0×15.0 mm^2. The camera and laser were connected to a digital delay generator (Berkeley Nucleonics, model 565), which controlled the timing of the laser illumination and image acquisition for the PIV measurements.

After PIV image acquisition, the PIV image pairs were processed by using a recursive two-frame cross-correlation algorithm to derive instantaneous flow velocity vectors. Although the first pass of the image processing operation used 64×64 pixel interrogation windows, the second pass used 32×32 pixel interrogation windows with 50% overlap of the interrogation windows to satisfy the Nyquist criterion. The derived instantaneous flow vectors were then validated by using a median filtering procedure to delete the outlier vectors and replace them with interpolated vectors based on the validated neighboring vectors. For the PIV measurements of the present study, typically only less than 1% of the velocity vectors in any given instantaneous PIV frames would be identified as the outlier vectors. Once the instantaneous flow velocity vectors (u_i, v_i) were determined, the distributions of the ensemble-averaged quantities such as averaged flow velocity and normalized in-plane turbulence kinetic energy

$$\mathrm{NTKE} = \frac{1}{2}\left(\overline{u'^2} + \overline{v'^2}\right)/U_\infty^2$$

could be obtained based on a sequence of 1000 realizations of instantaneous PIV measurements. The measurement uncertainty level for the flow velocity vectors was estimated to be within 3.0% for the present study.

III. Measurement Results and Discussions

A. Effects of Flow Compressibility and Blowing Ratio on the Film Cooling Effectiveness

Figure 3 shows typical PSP measurement results in terms of the film cooling effectiveness distributions downstream of the circular coolant injection hole in the middle of the test plate, with the blowing ratios being $M = 0.40$, 0.85, and 1.25, respectively. During the experiments, while the density ratio of the two streams was fixed at $DR \approx 1.5$ (i.e., CO_2 was used as the coolant stream for the PSP measurements), the Mach number of the mainstream flow was changed from $Ma = 0.07$ (i.e., low-speed, incompressible, flow) to $Ma = 0.70$ (i.e., compressible, transonic flow). It can be seen clearly that, even though the freestream speed of the mainstream flow was increased by a factor of 10 (i.e., increased from $Ma = 0.07$ to $Ma = 0.70$), both the distribution pattern and footprint length of the measured film cooling effectiveness maps over the test plate at different test conditions were found to be quite similar, as long as the blowing ratio of the test cases was set to be the same level. It suggests that the film cooling performance of the circular coolant injection seems to be almost independent of the Mach number of the mainstream flow, especially for the test cases with the blowing ratio relatively low (i.e., for the test cases of $M = 0.4$, as shown in Fig. 3a). The finding of the present study based on the PSP measurements was found to agree reasonably well with the conclusions reported by Gritsch et al. [7] and Liess [8], who conducted film cooling

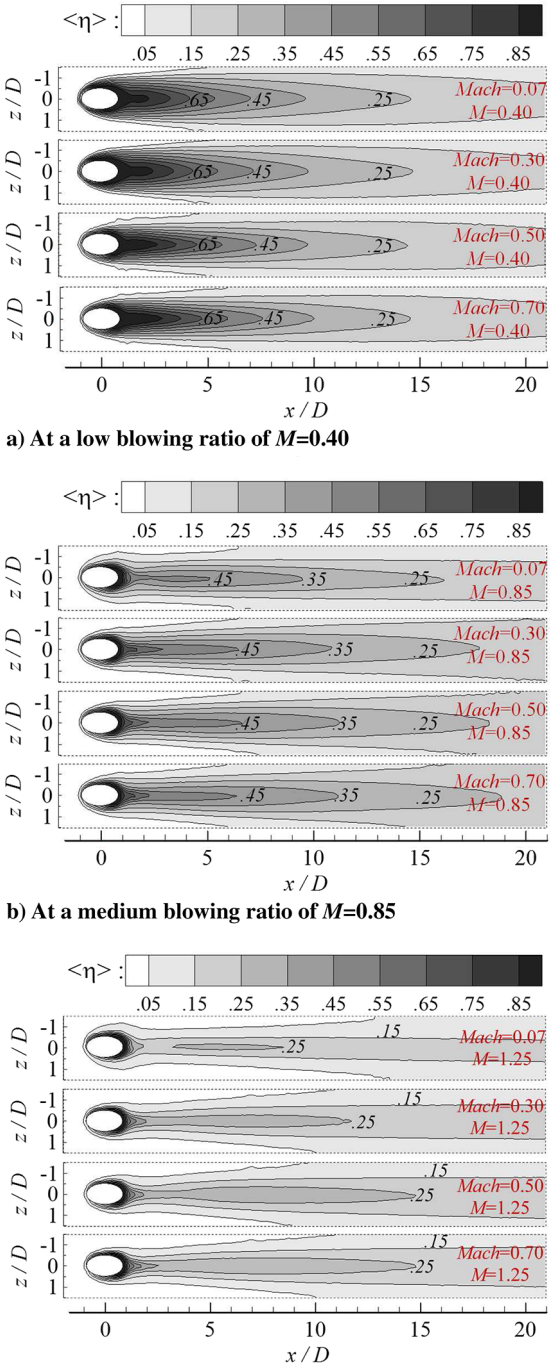

a) At a low blowing ratio of M=0.40

b) At a medium blowing ratio of M=0.85

c) At a high blowing ratio of M=1.25

Fig. 3 Measured cooling effectiveness distributions at different test conditions.

effectiveness measurements by using an infrared thermal imaging technique.

It can also be seen that the measured film cooling effectiveness distributions over the test plate would change dramatically as the blowing ratio of the test cases was increased from $M = 0.40$ (i.e., low blowing ratio) to $M = 1.25$ (i.e., high blowing ratio). At a relatively low blowing ratio (i.e., $M = 0.4$ case), the coolant stream out of the circular coolant injection hole was found to have a rather uniform and wide coverage over the surface of the test plate, especially in the near-field region downstream of the coolant injection hole. As the blowing ratio increased to $M = 0.85$ and $M = 1.25$, the contour lines of the regions with higher cooling effectiveness values were found to become much narrower in spanwise direction and shorter in the downstream direction. It indicated that the coolant stream exhausted from the coolant injection hole would lift off from the test plate and penetrate into the mainstream flow as a cross jet flow, resulting in poor film cooling protection to the surface of the test plate, which was revealed more clearly from the PIV measurements to be described later. Very similar scenarios of the film cooling were also reported by Baldauf et al. [2], who conducted film cooling effectiveness measurements by using an infrared thermal imaging system with the incoming mainstream flow being low-speed incompressible flow (i.e., $Ma < 0.2$).

Based on the measured film cooling effectiveness distributions as those shown in Fig. 3, the centerline cooling effectiveness profiles as well as the laterally averaged cooling effectiveness profiles were extracted, which could be used to reveal the effects of the flow compressibility and the blowing ratio on the performance of the film cooling over the surface of the test plate more clearly and quantitatively. Note that, although the centerline cooling effectiveness profiles referred the measured cooling effectiveness values along the centerline of the coolant injection hole (i.e., along the line of $Z/D = 0$ as shown Fig. 3), the laterally averaged cooling effectiveness data were determined by averaging the film cooling effectiveness data along the lateral direction over one full period of the hole spacing (i.e., in the region of $-1.5 \le Z/D \le 1.5$) at each downstream location behind the coolant injection hole. Figure 4 shows the profiles of the centerline cooling effectiveness and the laterally averaged cooling effectiveness as a function of the downstream distance away from the coolant injection hole at the blowing ratios of $M = 0.40$ (low), 0.85 (medium), and 1.25 (high), respectively. Only the measurement data for the test cases with the mainstream flow being incompressible low-speed flow (i.e., the baseline case of $Ma = 0.07$, as indicated in solid lines) and compressible, transonic flow (i.e., $Ma = 0.70$ case, as indicated in dashed lines) were given here for conciseness. It can be seen clearly that, at the relatively low blowing ratio of $M = 0.40$, the film cooling effectiveness profiles for the two compared cases were found to be almost identical over the entire region of interest. It indicates that flow compressibility had almost no effect on the film cooling effectiveness over the surface of interest.

As the blowing ratio increased to $M = 0.85$ (medium) and $M = 1.25$ (high), the absolute values of the film cooling effectiveness were found to be much smaller at the near field of the coolant injection hole, in comparison with those of the baseline case at a low blowing ratio of $M = 0.40$. However, in the further downstream region of $x/D > 10$, the measured cooling effectiveness values for $M = 0.85$ case were found to be marginally higher than those of the baseline case at $M = 0.40$. More specifically, although the centerline cooling effectiveness for the transonic speed case ($Ma = 0.70$) with $M = 0.85$ was found to be only ~3% higher than that of the incompressible case ($Ma = 0.07$) at a blowing ratio of $M = 0.40$ at the downstream location of $x/D = 15$, the laterally averaged cooling effectiveness was found to be ~14% higher at the same downstream location. The observed better cooling effectiveness at the further downstream region could be particularly interesting for the turbine design, as there was often a need to avoid suction-side cooling injection holes in high Mach regions. As a result, there are often long cooling runs ($x/D \gg 10$) past the last row of effusion cooling holes on the suction side of the turbine blades.

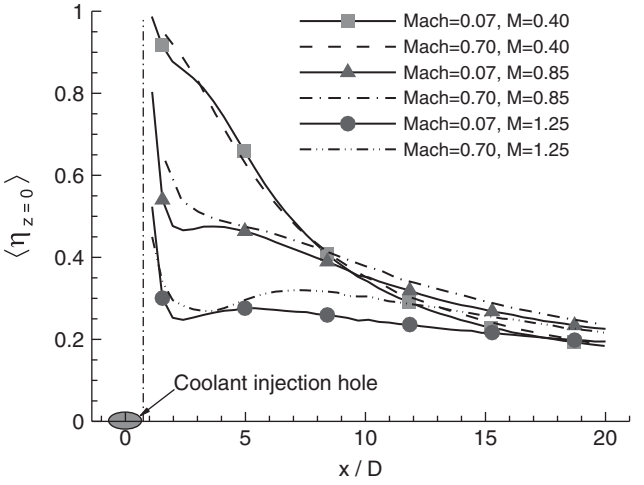

a) Centerline cooling effectiveness profiles

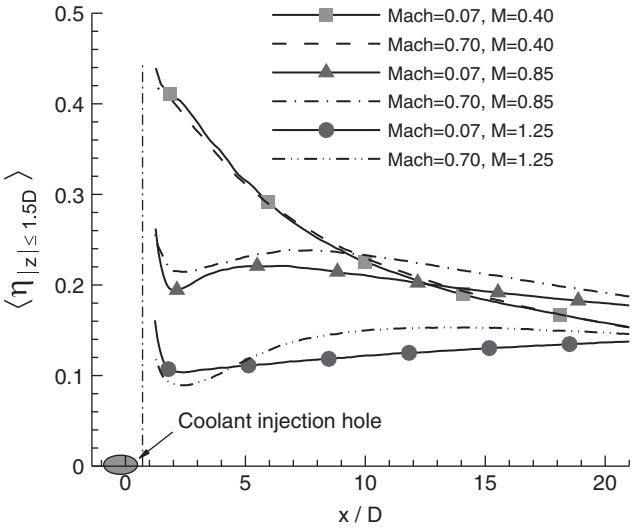

b) Laterally averaged cooling effectiveness profiles

Fig. 4 Measured cooling effectiveness profiles with $Ma = 0.07$ and 0.70.

It can also be seen that the effectiveness values for the test cases with transonic flow (i.e., $Ma = 0.70$) were found to become slightly higher than those of the baseline cases, with the mainstream being incompressible flow (i.e., $Ma = 0.07$) at the same blowing ratios. The largest differences between the two compared cases were found to be within ~15% for the centerline cooling effectiveness profiles and 25% for the laterally averaged profiles at the blowing ratio of $M = 1.25$.

To evaluate the overall effects of the flow compressibility on the film cooling effectiveness over the protected surface at different blowing ratios more quantitatively, a new parameter, named the area-averaged film cooling effectiveness $\eta_{\text{area-averaged}}$ is introduced, which is defined as follows:

$$\overline{\eta}_{\text{area-averaged}} = \frac{\iint \eta(x, z)\, \mathrm{d}A}{A} \tag{3}$$

where $\eta(x, z)$ is the measured film cooling effectiveness data over the test plate; and A is the area of interest, which is over one full period of the hole spacing (i.e., in the rectangular window of $1 \le X/D \le 20$ and $-1.5 \le Z/D \le 1.5$) for the present study. Figure 5 shows the measured area-averaged film cooling effectiveness data as a function of the Mach number of the mainstream flow at three different blowing ratios. As shown clearly in the plot, the measured area-averaged cooling effectiveness is found to be almost a constant value (i.e., the differences among different test cases are found to be within 3%)

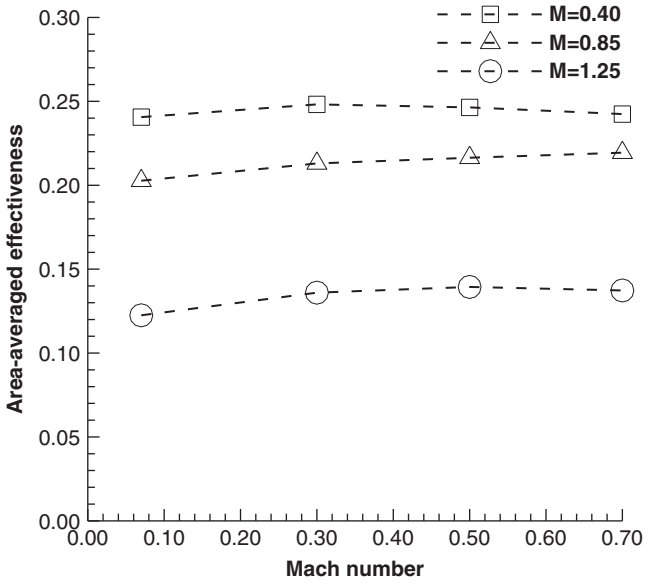

Fig. 5 Area-averaged film cooling effectiveness as a function of the Mach number of the mainstream flow at different blowing ratios.

at the relatively low blowing ratio of $M = 0.40$. It confirms again that the film cooling effectiveness is almost independent of the flow compressibility at the relatively low blowing ratio of $M = 0.40$. As the blowing ratio increases to much higher values of $M = 0.85$ and 1.25, marginal improvements in the overall film cooling effectiveness can be observed for the test cases, with mainstream flow having higher Mach numbers. More specifically, the area-averaged cooling effectiveness for the test case with the mainstream being a transonic, compressible flow (i.e., $Ma = 0.70$ case) will be about 13% greater than that of the test case with the mainstream flow being low-speed incompressible (i.e., $Ma = 0.07$ case) at the medium blowing ratio of $M = 0.85$. It will become ~15% better at the high blowing ratio of $M = 1.25$.

The phenomenon, shown in Figs. 3–5, is believed to be caused by the relatively small convective Mach numbers of the present study. As shown clearly in Table 1, the convective Mach numbers for most of the test conditions fall into a low compressibility regime with $Ma_{c1,2} \leq 0.3$ and $\theta_0 = 1$. In this regime, the effects of compressibility on film cooling effectiveness are generally very small and the high-speed flow can be approximately treated as an incompressible low-speed flow. Thus, the flow compressibility has almost no effect on the effectiveness of film cooling at the low blowing ratio of $M = 0.4$. Nevertheless, as the blowing ratios increase to $M = 0.85$ and 1.25, the magnitudes of convective Mach number are found to become bigger as the mainstream Mach number rises from $Ma = 0.07$ to $Ma = 0.70$. As reported by Dellimore et al. [10], increasing the convective Mach number will decrease the growth rate of the compressible shear layer, leading to improved film cooling effectiveness. Therefore, the slight improvement in cooling effectiveness for high blowing ratio cases is believed to be caused by the increasing compressibility effects on film cooling as the Mach number of the mainstream increases.

Figure 6 shows some typical PIV measurement results in terms of ensemble-averaged flow velocity fields near the coolant injection hole in the centerplane of the test plate, which can be used to elucidate further insight into the underlying physics pertinent to the experimental observations described previously. Although PIV measurements are conducted for more test cases, only the measurement results with the mainstream flow being either incompressible (i.e., baseline case of $Ma = 0.07$, left figure) or compressible flow of $Ma = 0.50$ (i.e., right figure) are presented

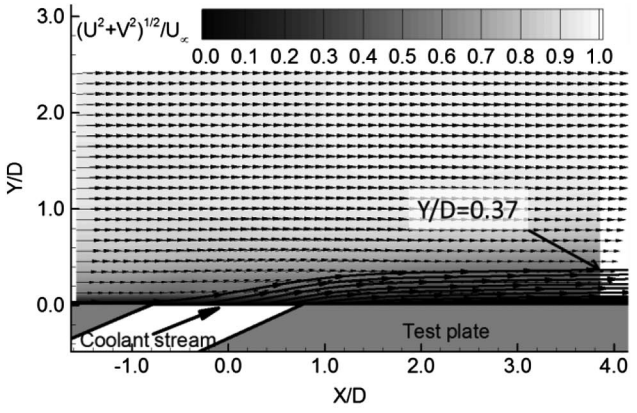

a) Test case with *Ma*=0.07; *M*=0.40

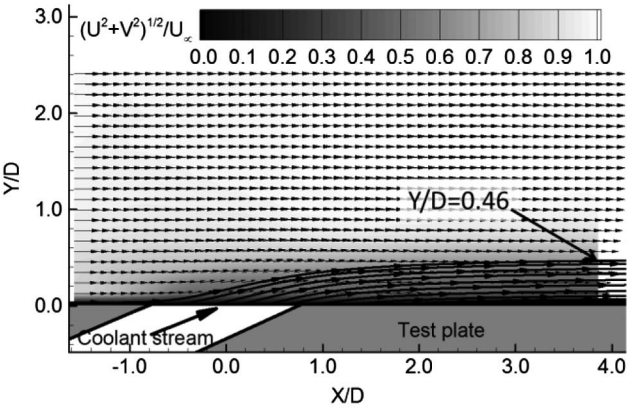

b) Test case with *Ma*=0.50; *M*=0.40

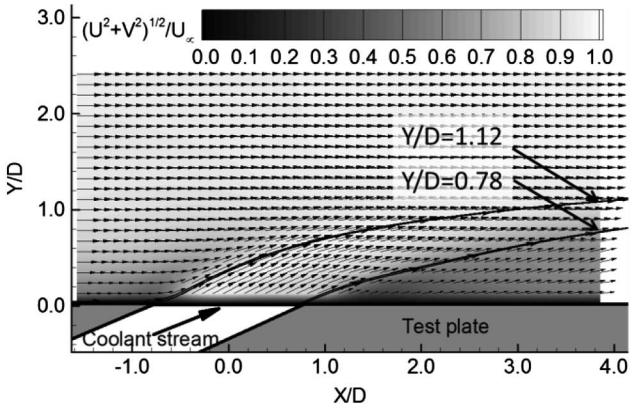

c) Test case with *Ma*=0.07; *M*=1.25

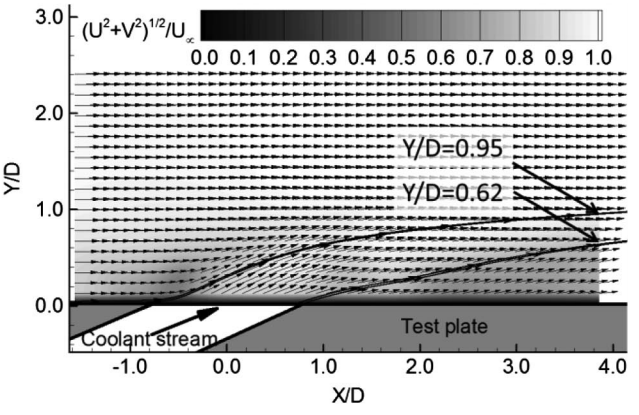

d) Test case with *Ma*=0.50; *M*=1.25

Fig. 6 PIV measurement results at different test conditions.

here for conciseness. As shown clearly in Figs. 6a and 6b, at the relatively low blowing ratio of $M = 0.40$, the coolant stream out of the injection hole is found to be able to stay attached to the surface of the test plate to form a coolant film layer over the protected surface for both the low-speed incompressible baseline case (i.e., $Ma = 0.07$) and compressible flow case of $Ma = 0.50$. It results in a rather good film cooling protection to the surface of interest (i.e., high film cooling effectiveness values and wide coverage of the coolant stream in the spanwise direction, especially in the near-field region downstream the coolant injection hole), as revealed quantitatively from the film cooling effectiveness distributions given in Fig. 3a. By carefully inspecting the streamlines of the coolant stream flow over the test plate, it can be found that the coolant stream exhausted from the injection hole seems to form a thicker coolant layer over the surface of the test plate for the test case with the mainstream having a higher Mach number (i.e., the thickness of the coolant layer over the test plate is found to reach $Y/D \approx 0.46$ at the downstream location of $X/D \approx 3.8$ for the $Ma = 0.5$ case, in comparison with $Y/D \approx 0.37$ for the baseline case with the mainstream being incompressible low-speed flow of $Ma = 0.07$). As a result, the film cooling performance over the test plate is expected to be slightly better for the test case with the mainstream flow having a higher Mach number (i.e., $Ma = 0.50$ case), which is confirmed quantitatively from the measured area-averaged film cooling effectiveness data given in Fig. 5.

At the high blowing ratio of $M = 1.25$, the behavior of the coolant stream out of the injection hole was found to be significantly different from that of the test cases with the low blowing ratio of $M = 0.4$. As revealed in Figs. 6c and 6d, the coolant jet stream was found to lift off from the surface of the test plate and penetrate deeply into the mainstream flow as a cross jet flow, resulting in poor film cooling performance over the surface of the test plate (i.e., much smaller film cooling effectiveness values and narrower coverage of the coolant footprints in the spanwise direction), as revealed clearly in the measured cooling effectiveness distributions shown in Fig. 3. Although the flow features revealed from the ensemble-averaged flow velocity distributions were found to be very similar in general for the two compared cases, the liftoff of the coolant stream was found to become more severe for the test case with the mainstream flow being incompressible low-speed flow (i.e., the baseline case of $Ma = 0.07$), in comparison with that of the compressible case of $Ma = 0.50$. Although the streamlines starting from the leading and trailing edges of the coolant injection hole were found to reach up to $Y/D \approx 1.12$ and $Y/D \approx 0.78$ for the $Ma = 0.07$ case at the exit of the PIV measurement window (i.e., at the downstream location of $X/D \approx 3.8$), they were only at $Y/D \approx 0.95$ and $Y/D \approx 0.62$ for the $Ma = 0.70$ case. It indicates that the coolant stream would remain slightly closer to the surface of the test plate for the $Ma = 0.5$ case, in comparison to that of the baseline case of $Ma = 0.07$. As a result, the measured film cooling effectiveness for the test case with a higher Mach number of mainstream flow was found to become marginally better than of the baseline case with incompressible low-speed mainstream flow of $Ma = 0.07$.

B. Effects of Density Ratio of Coolant to Mainstream on the Film Cooling Performance

As described previously, most of previous experimental studies on film cooling were performed to quantify the heat transfer process associated with film cooling by measuring the wall temperature over the surface of interest; the corresponding density ratios between the coolant and mainstream ($DR = \rho_c/\rho_\infty$) were usually quite small (i.e., approximately 1.0) due to the limited temperature differences between the two streams used in those heat transfer studies [2,12–14]. However, the density ratios between the hot mainstream and coolant flow in a real gas turbine engine was usually much higher (i.e., in the range of $1.5 \sim 2.0$) due to the significant temperature differences between the two streams [14–16]. Furthermore, the majority of the previous experimental studies on film cooling were conducted with the coolant and mainstream being low-speed incompressible flows (i.e., $Ma < 0.2$); the effects of the density ratio on the performance of film cooling have not been fully explored, especially at the test conditions with the coolant and mainstream being compressible, transonic flows. In the present study, an experimental study was also performed to investigate the effects of the density ratio between the coolant and mainstream on the film cooling effectiveness with the two stream flows being transonic, compressible to better represent the incoming flow conditions in a realistic gas turbine engine.

In the present study, by using either N_2, CO_2, or a mixture of SF_6 and CO_2 as the coolant gas and oxygen-containing air as the mainstream for the PSP measurements, the density ratios between the coolant and mainstreams were changed to $DR \approx 1.0$, 1.5, and 2.0, respectively. Figure 7 shows the measured film cooling effectiveness distributions over the test plate with the mainstream flow being a compressible, transonic flow (i.e., $Ma = 0.70$) and the blowing ratios of the test cases being $M = 0.40$, 0.85, and 1.25, respectively. The effects of the density ratio on the film cooling performance were revealed clearly from the comparisons of the measurement results. It could be seen clearly that, at the relatively low blowing ratio of $M = 0.40$, the measured film cooling effectiveness distributions were found to be very similar, despite the different density ratios for the test cases. The distribution pattern of the film cooling effectiveness maps indicated that the coolant stream would remain attached to the surface of the test plate, as revealed clearly from PIV measurement results given in Fig. 6a. However, as the blowing ratio

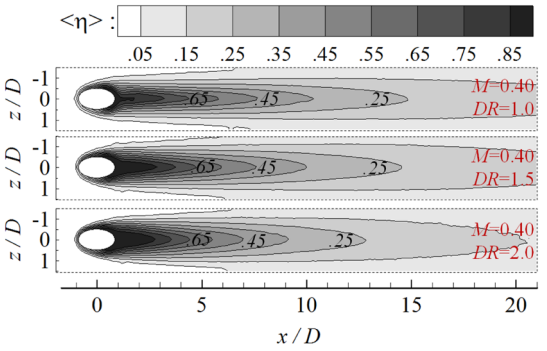

a) At low blowing ratio of M=0.40

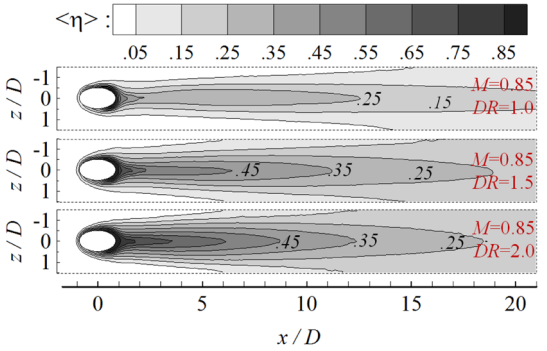

b) At medium blowing ratio of M=0.85

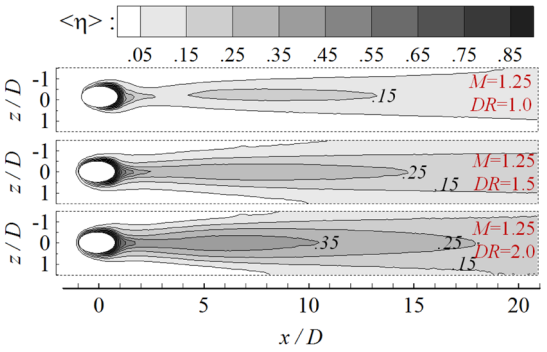

c) At high blowing ratio of M=1.25

Fig. 7 Measured cooling effectiveness distributions at different density ratios with the mainstream being transonic, compressible flow (i.e., $Ma = 0.70$).

became greater than 0.85 (i.e., $M \geq 0.85$), both the absolute values and distribution pattern of the film cooling effectiveness contour lines were found to depend upon the density ratio of the test case substantially. A denser coolant flow was found to result in a better performance of film cooling over the surface of interest.

Based on the film cooling effectiveness distributions given in Fig. 7, the profiles of the film cooling effectiveness along the center line of the circular coolant injection hole and the laterally averaged cooling effectiveness can be extracted, which are shown in Fig. 8. Only the measurement data for the test cases with the blowing ratio of $M = 0.40$ (i.e., low blowing ratio) and $M = 1.25$ (i.e., high blowing ratio) are shown in the plot for conciseness. Figure 9 shows the measured area-averaged film cooling effectiveness values $\overline{\eta}_{\text{area-averaged}}$ as a function of the coolant to mainstream density ratios for the test cases with the mainstream being compressible, transonic mainstream flow (i.e., $Ma = 0.70$) versus those of baseline cases with the mainstream being incompressible low-speed flow (i.e., $Ma = 0.07$). It is apparent that, because the coolant stream will remain attached to the surface of the test plate at the relatively low blowing ratio of $M = 0.40$, the density ratio of the coolant to mainstream flow is found to have only marginal effects on the film cooling effectiveness profiles. As shown clearly in Fig. 9, at the relatively low blowing ratio of $M = 0.40$, the area-averaged cooling effectiveness $\overline{\eta}_{\text{area-averaged}}$ over the surface of the interest is found to increase about 10%, with the density ratio of the two streams increasing from $DR = 1.0$ to $DR = 2.0$. As the blowing ratio becomes greater than 0.85 (i.e., $M > 0.85$), the coolant stream out of

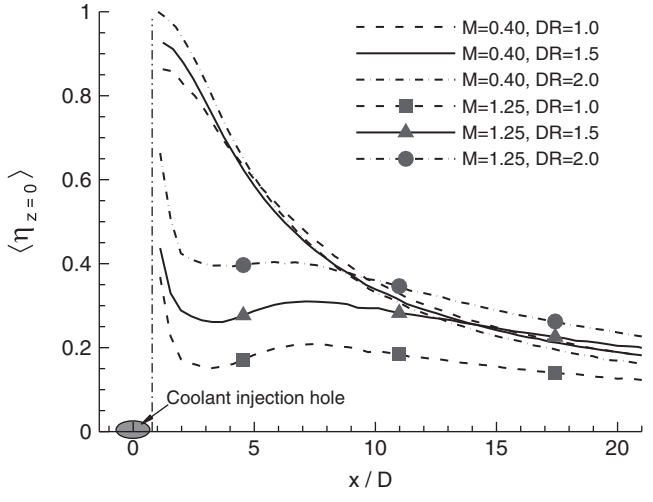

a) Centerline cooling effectiveness profiles

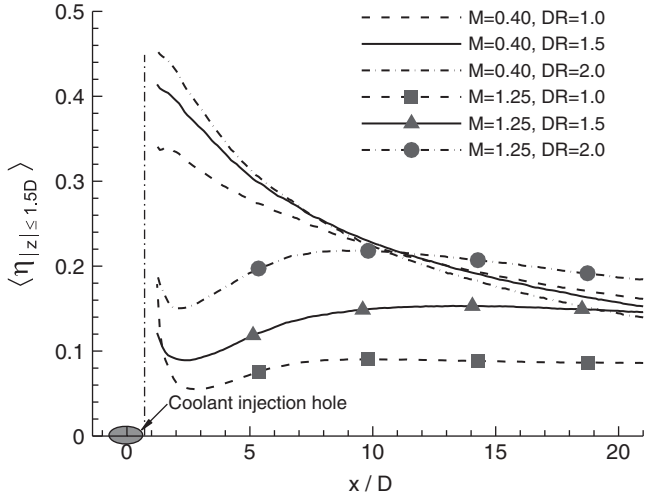

b) Laterally averaged cooling effectiveness profiles

Fig. 8 Effects of the density ratio DR on the film cooling effectiveness with the mainstream being compressible, transonic flow (i.e., $Ma = 0.70$).

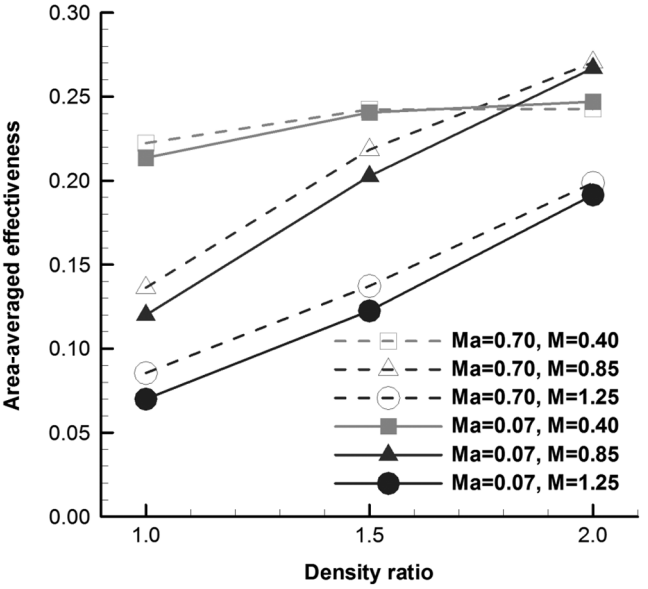

Fig. 9 Effects of density ratio DR on the area-averaged cooling effectiveness with the mainstream flow being incompressible (i.e., $Ma = 0.07$) vs those of compressible (i.e., $Ma = 0.70$).

the circular coolant injection hole will lift off from the surface of the test plate and penetrate into the mainstream flow, as shown in the PIV measurements given in Fig. 6. The density ratio of the two streams is found to affect the performance of film cooling over the surface of the test plate substantially. As shown clearly in Fig. 8, at the blowing ratio of $M = 1.25$, the measured values of the film cooling effectiveness for both the centerline and lateral-averaged profiles are found to become much greater as the density ratio of the test case increases. More quantitatively, the area-averaged film cooling effectiveness $\overline{\eta}_{\text{area-averaged}}$ is found to increase by a factor of about 2.5, with the density ratio of the two streams increasing from $DR = 1.0$ to $DR = 2.0$, as shown clearly in Fig. 9. This can be explained by the fact that, at a fixed blowing ratio level, the momentum of the coolant jet stream will be lower for a denser coolant (i.e., $I = M^2/DR$). Thus, the coolant stream out of the circular injection hole will tend to stay much closer to the surface of the test plate than a lighter coolant flow, resulting in a better film cooling protection to the surface of interest. Similar findings were also reported by Johnson et al. [32], with the mainstream flow being incompressible low-speed flow (i.e., $Ma < 0.20$).

Based on the quantitative measurements shown in Fig. 9, the influence of the flow compressibility on the density ratio effects is also revealed quantitatively. It can be seen clearly that, at the relatively low density ratio of $DR = 1.0$, the area-averaged cooling effectiveness values for the test cases with compressible, transonic mainstream flows (i.e., $Ma = 0.70$) are found to be marginally higher than those of the baseline cases with low-speed incompressible mainstream flows (i.e., $Ma = 0.07$). As the density ratios increase to $DR = 1.5$ and $DR = 2.0$, the differences in the measured area-averaged cooling effectiveness between the compressible and incompressible flow cases are found to become smaller and smaller. It indicates that, at a high density ratio level, similar to those in realistic gas turbines, the film cooling effectiveness measurements with the mainstream being low-speed incompressible flow (i.e., $Ma = 0.07$) will be a reasonably good estimation to that with transonic, compressible mainstream flow (i.e., $Ma = 0.70$). In summary, although the density ratio of the coolant to the mainstream flows is found to affect the film cooling effectiveness substantially for the test cases with relatively high blowing ratios, the sensitivity of the film cooling performance to the Mach number of the mainstream flow is found to be lessened for the test cases with higher density ratios.

It is worth noting that, with the blowing ratio M being fixed, varying the density ratio DR also implies a variation of velocity ratio

(VR). To elucidate the effects of the VR and DR on film cooling performance more clearly, the measured film cooling effectiveness behind the coolant injection holes with a matched VR at varying DR are shown in Fig. 10. It can be seen that, with a matched velocity ratio of $VR = 0.40$, the film cooling effectiveness values for the case with $DR = 2.0$ are found to be higher than those of the $DR = 1.5$ case, which is consistent with the conclusion revealed in Figs. 8 and 9. Increasing the VR to 0.85, the absolute values of the cooling effectiveness are found to become smaller, in comparison to those of the $VR = 0.4$ cases, as expected. Although the cooling effectiveness for the $DR = 1.5$ case is found to be better than that of the $DR = 1.0$ case at the further downstream region (i.e., $x/D > 7.0$), the center line and the laterally averaged effectiveness values of the $DR = 1.0$ case are found to be slightly higher than those of the $DR = 1.5$ case in the region near the coolant injection hole, which is contradictory to the finding described previously. Such measurement results indicate that the VR may affect the film cooling effectiveness greatly, especially in the region near the coolant injection hole. By comparing the cooling effectiveness profiles of the test cases with the matched density ratio of $DR = 1.5$, the film cooling effectiveness for the test case with $VR = 0.40$ is found to be significantly higher than that of $VR = 0.83$ case in the region near the coolant injection hole (i.e., $x/D \leq 10$). The profiles are found to converge slowly in the further downstream region (i.e., $x/D > 10$). This can be explained by the fact that the coolant stream will take off from the surface of the test plate at $VR = 0.83$, leading to deteriorated film cooling performance. In summary, although the VR will be a dominant factor to affect the performance of film cooling in the near-hole region (i.e., $x/D < 10$), the relative impact of DR and the VR begins to converge at the further downstream region. DR may have a bigger influence on film cooling in the far downstream region.

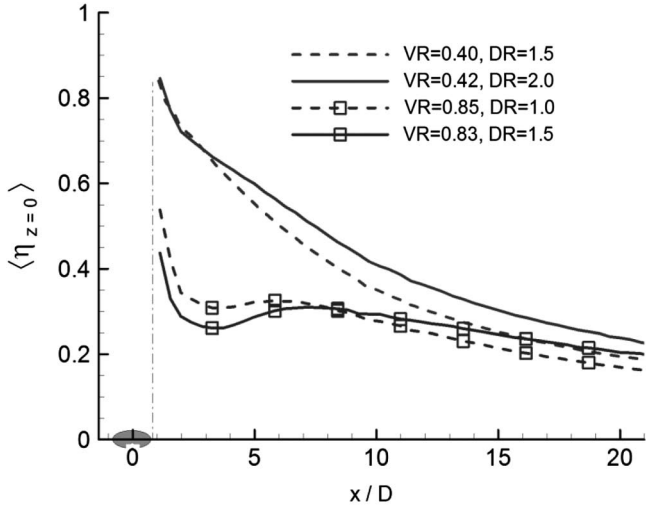

a) Centerline cooling effectiveness profiles

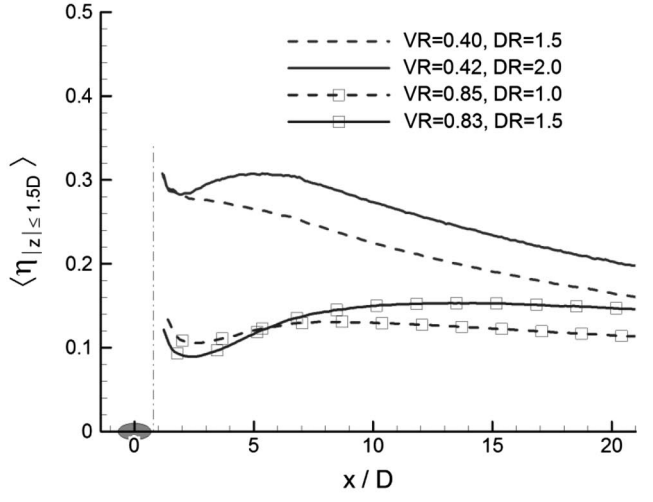

b) Laterally averaged cooling effectiveness profiles

Fig. 10 Measured cooling effectiveness results with matched velocity ratio at $Ma = 0.70$.

IV. Conclusions

An experimental investigation was performed to evaluate the effects of the flow compressibility and density ratio of the coolant to mainstream flows on the performance of film cooling in a transonic wind tunnel available at Iowa State University. During the experiments, the coolant stream was injected from an array of circular holes at an inclined injection angle of $\alpha = 35$ deg related to a mainstream flow. Although a high-resolution particle image velocimetry system was used to quantify the turbulent mixing process between the mainstream flow and the cross coolant jet stream at different test conditions, a pressure-sensitive paint technique was used to map the corresponding adiabatic film cooling effectiveness distributions over the surface of the test plate based on a mass flux analog to traditional temperature-based cooling effectiveness measurements. The effects of the flow compressibility (i.e., as indicated by the Mach number of the mainstream flow $Ma = 0.07$, 0.30, 0.50, and 0.70) and the density ratios of the coolant to mainstream flows (i.e., $DR = 1.0$, 1.5, and 2.0) on the film cooling effectiveness over the surface of interest at different blowing ratios (i.e., mass flux ratio $M = 0.40$, 0.85, and 1.25) were examined in detail based on the quantitative PSP and PIV measurements.

It was found that the coolant jet streams out of the circular injection holes would remain attached to the surface of the test plate at a relatively low blowing ratio of $M = 0.40$, resulting in a good film cooling protection over the surface of interest. The flow compressibility was found to have almost no effects on the film cooling effectiveness over the surface of interest (i.e., the differences were found to be within 3% for the test cases, with the Mach number of the mainstream changing from $Ma = 0.07$ to $Ma = 0.70$). At relatively high blowing ratios (i.e., $M > 0.85$), the coolant jet stream would lift off from the surface of the test plate, causing a much poorer film cooling protection to the surface of the test plate. The film cooling effectiveness for the test cases with the mainstream being compressible flows (i.e., the test cases of $Ma > 0.3$) were found to become marginally better than that of the baseline case with the mainstream being incompressible low-speed flow (i.e., $Ma = 0.07$ case). More specifically, the area-averaged cooling effectiveness for the test cases with the mainstream being compressible, transonic flow (i.e., $Ma = 0.70$ case) was found to be ~13% better than that of the baseline case at the medium blowing ratio of $M = 0.85$. It became ~15% better at the high blowing ratio of $M = 1.25$. This was believed to be caused by the increased compressibility effects on film cooling effectiveness as the Mach number of the mainstream increased for the test cases with high blowing ratios. As revealed clearly in the PIV measurements, the penetration of the coolant jet streams exhausted from the coolant injection holes would become less severe for the test cases with a higher Mach number of the mainstream flow, in comparison to the baseline case with a low-speed incompressible mainstream flow. Less penetration of the coolant jet into the mainstream flow would lead to a better film cooling effectiveness over the surface of interest.

It was also found that the coolant to mainstream density ratio would have limited effects on the film cooling performance as the coolant jet stream still was able to stay attached to the surface at the relatively low blowing ratio of $M = 0.40$. The area-averaged effectiveness over the surface of interest was found to improve about 10% with the density ratio increasing from $DR = 1.0$ to $DR = 2.0$. However, when the coolant stream was lifted off the surface of the test plate at relatively high blowing ratios (i.e. $M > 0.85$), the density ratio of the coolant to the mainstream was found to affect the film cooling effectiveness substantially. A denser coolant flow would result in a better film cooling protection to the surface of interest. More specifically, the area-averaged film cooling effectiveness over the surface of interest was found to increase by a factor of about 2.5,

with the density ratio of the two streams increasing from $DR = 1.0$ to $DR = 2.0$. Although the density ratio of the coolant to the mainstream flows was found to affect the film cooling performance significantly at relatively high blowing ratios, the sensitivity of the film cooling performance to the flow compressibility was found to be lessened as the density ratio of the coolant to the mainstream increased. It was also found that, although the VR would be a dominant factor to affect the performance of film cooling in the near-hole region (i.e., $x/D < 10$), the relative impact of DR and the VR began to converge at the further downstream region. DR might have a greater influence on film cooling in the far downstream region.

It should also be noted that the primary objective of this fundamental study was to elucidate the underlying physics associated with the effects of flow compressibility and the density ratio of the coolant to mainstream flows on the film cooling effectiveness pertinent to the film cooling of hot section components of gas turbines. Although the findings derived from the present study were believed to be helpful to improve the understanding of the underlying physics and to evaluate the effects of flow compressibility and density ratios on the film cooling performance, much extensive work is still needed to quantify the effects of relevant key parameters, such as the velocity ratio and momentum ratio of the coolant to mainstream flows; the associated aerodynamic losses and heat transfer coefficients; and the pressure gradients, as well as the surface curvatures of the turbine blades, on the film cooling performance, in order to elucidate underlying physics to explore/optimize design paradigms for a better film cooling protection to hot section components of gas turbines.

Acknowledgments

The authors would like to thank Bill Rickard, Andrew Jordan, and Jim Benson of Iowa State University for their assistance with the experimental setup of the experiments, as well as conducting the experiments.

Reference

[1] Goldstein, R. J., Eckert, E. R. G., and Burggraf, F., "Effects of Hole Geometry and Density on Three-Dimensional Film Cooling," *International Journal of Heat and Mass Transfer*, Vol. 17, No. 5, 1974, pp. 595–607. doi:10.1016/0017-9310(74)90007-6

[2] Baldauf, S., Schulz, A., and Wittig, S., "High-Resolution Measurements of Local Effectiveness from Discrete Hole Film Cooling," *Journal of Turbomachinery*, Vol. 123, No. 4, 2001, pp. 758–765. doi:10.1115/1.1371778

[3] Baldauf, S., Scheurlen, M., Schulz, A., and Wittig, S., "Correlation of Film-Cooling Effectiveness from Thermographic Measurements at Engine Like Conditions," *Journal of Turbomachinery*, Vol. 124, No. 4, 2002, pp. 686–698. doi:10.1115/1.1504443

[4] Bogard, D. G., "Airfoil Film Cooling," *The Gas Turbine Handbook*, National Energy Technology Lab., Morgantown, WV, 2006, pp. 309–318, Sec. 4.2.1.

[5] Bogard, D. G., and Thole, K. A., "Gas Turbine Film Cooling," *Journal of Propulsion and Power*, Vol. 22, No. 2, 2006, pp. 249–270. doi:10.2514/1.18034

[6] Bunker, R. S., "A Review of Shaped Hole Turbine Film-Cooling Technology," *Journal of Heat Transfer*, Vol. 127, No. 4, 2005, pp. 441–453. doi:10.1115/1.1860562

[7] Gritsch, M., Schulz, A., and Wittig, S., "Adiabatic Wall Effectiveness Measurements of Film Cooling Holes with Expanded Exits," *Journal of Turbomachinery*, Vol. 120, No. 3, 1998, pp. 549–556. doi:10.1115/1.2841752

[8] Liess, C., "Experimental Investigation of Film Cooling with Ejection from a Row of Holes for the Application to Gas Turbine Blades," *Journal of Engineering for Power*, Vol. 97, No. 1, 1975, pp. 21–27. doi:10.1115/1.3445904

[9] Repukhov, V. M., "Effects of Compressibility and Nonisothermal Conditions on the Performance of Film Cooling," *Journal of Engineering Physics and Thermophysics*, Vol. 19, No. 5, 1970, pp. 1401–1408. doi:10.1007/BF00833476

[10] Dellimore, K. H., Marshall, A. W., and Cadou, C. P., "Influence of Compressibility on Film-Cooling Performance," *Journal of Thermophysics and Heat Transfer*, Vol. 24, No. 3, 2010, pp. 506–515. doi:10.2514/1.45092

[11] Parthasarathy, K., and Zakkay, V., "An Experimental Investigation of Turbulent Slot Injection at Mach 6," *AIAA Journal*, Vol. 8, No. 7, 1970, pp. 1302–1307. doi:10.2514/3.5889

[12] Kunze, M., Preibisch, S., Vogeler, K., Landis, K., and Heselhaus, A., "A New Test Rig for Film Cooling Experiments on Turbine Endwalls," *ASME Turbo Expo 2008: Power for Land, Sea, and Air*, American Society of Mechanical Engineers, Fairfield, NJ, 2008, pp. 989–998. doi:10.1115/GT2008-51096

[13] Wright, L. M., McClain, S. T., and Clemenson, M. D., "Effect of Density Ratio on Flat Plate Film Cooling with Shaped Holes Using PSP," *Journal of Turbomachinery*, Vol. 133, No. 4, 2011, Paper 041011. doi:10.1115/1.4002988

[14] Han, J., Dutta, S., and Ekkad, S., *Gas Turbine Heat Transfer and Cooling Technology*, 1st ed., CRC Press, Boca Raton, FL, 2000, p. 186.

[15] Pietrzyk, J. R., Bogard, D. G., and Crawford, M. E., "Effects of Density Ratio on the Hydrodynamics of Film Cooling," *ASME 1989 International Gas Turbine and Aeroengine Congress and Exposition*, American Society of Mechanical Engineers, Fairfield, NJ, 1989, Paper V004T08A018. doi:10.1115/89-GT-175

[16] Sinha, A. K., Bogard, D. G., and Crawford, M. E., "Film-Cooling Effectiveness Downstream of a Single Row of Holes with Variable Density Ratio," *Journal of Turbomachinery*, Vol. 113, No. 3, 1991, pp. 442–449. doi:10.1115/1.2927894

[17] Hansmann, T., Wilhelmi, H., and Bohn, D., "An Experimental Investigation of the Film-Cooling Process at High Temperatures and Velocities," *5th AIAA/DGLR International Aerospace Planes and Hypersonics Technologies Conference*, AIAA Paper 1993-5062, 1993.

[18] Pedersen, D. R. D., Eckert, E. R. G., and Goldstein, R. J., "Film Cooling with Large Density Differences Between the Mainstream and the Secondary Fluid Measured by the Heat-Mass Transfer Analogy," *Journal of Heat Transfer*, Vol. 99, No. 4, 1977, pp. 620–627.

[19] Maqbool, D., Collett, M. D., Dellimore, K., Ruf, J. H., and Cadou, C. P., "Measurements of Film Cooling Performance in Supersonic Environments," *52nd AIAA Aerospace Sciences Meeting*, AIAA Paper 2014-0701, 2014.

[20] Urban, W. D., and Mungal, M. G., "Planar Velocity Measurements in Compressible Mixing Layers," *Journal of Fluid Mechanics*, Vol. 431, March 2001, pp. 189–222. doi:10.1017/S0022112000003177

[21] Hall, J. L., "An Experimental Investigation of Structure, Mixing and Combustion in Compressible Turbulent Shear Layers," Ph.D. Dissertation, California Inst. of Technology, Pasadena, CA, 1991.

[22] Rossman, T., Mungal, M. G., and Hanson, R., "An Experimental Investigation of High Compressibility Non-Reacting Mixing Layers," AIAA Paper 2000-0663, 2000.

[23] Rossmann, T., "An Experimental Investigation of High Compressibility Mixing Layers," Ph.D. Dissertation, Stanford Univ., Stanford, CA, 2001.

[24] Zhou, W., Johnson, B., and Hu, H., "An Experimental Study of Compressibility Effects on the Film Cooling Effectiveness Using PSP and PIV Techniques," *53rd AIAA Aerospace Sciences Meeting*, AIAA Paper 2015-0352, 2015. doi:10.2514/6.2015-0352

[25] Dellimore, K. H., "Modeling and Simulation of Mixing Layer Flows for Rocket Engine Film Cooling," Ph.D. Dissertation, Univ. of Maryland, College Park, MD, 2010.

[26] Papamoschou, D., and Roshko, A., "The Compressible Turbulent Shear Layer: An Experimental Study," *Journal of Fluid Mechanics*, Vol. 197, Dec. 1988, pp. 453–477. doi:10.1017/S0022112088003325

[27] Wright, L. M., Gao, Z., Varvel, T. A., and Han, J. C., "Assessment of Steady State PSP, TSP, and IR Measurement Techniques for Flat Plate Film Cooling," *ASME 2005 Summer Heat Transfer Conference collocated with the ASME 2005 Pacific Rim Technical Conference and Exhibition on Integration and Packaging of MEMS, NEMS, and Electronic Systems*, American Society of Mechanical Engineers, Fairfield, NJ, 2005, pp. 37–46. doi:10.1115/HT2005-72363

[28] Eckert, E. R. G., "Similarity Analysis of Model Experiments for Film Cooling in Gas Turbines," *Wärme-und Stoffübertragung*, Vol. 27, No. 4, 1992, pp. 217–223. doi:10.1007/BF01589919

[29] Shadid, J. N., and Eckert, E. R. G., "The Mass Transfer Analogy to Heat Transfer in Fluids with Temperature-Dependent Properties," *Journal of Turbomachinery*, Vol. 113, No. 1, 1991, pp. 27–33. doi:10.1115/1.2927734

[30] Han, J. C., and Rallabandi, A., "Turbine Blade Film Cooling Using PSP Technique," *Frontiers in Heat and Mass Transfer*, Vol. 1, No. 1, 2010, pp. 1–21. doi:10.5098/hmt.v1.1.3001

[31] Yang, Z., and Hu, H., "Study of Trailing-Edge Cooling Using Pressure Sensitive Paint Technique," *Journal of Propulsion and Power*, Vol. 27, No. 3, 2011, pp. 700–709. doi:10.2514/1.B34070

[32] Johnson, B., Tian, W., Zhang, K., and Hu, H., "An Experimental Study of Density Ratio Effects on the Film Cooling Injection from Discrete Holes by Using PIV and PSP Techniques," *International Journal of Heat and Mass Transfer*, Vol. 76, May 2014, pp. 337–349. doi:10.1016/j.ijheatmasstransfer.2014.04.028

[33] Bell, J. H., Schairer, E. T., Hand, L. A., and Mehta, R. D., "Surface Pressure Measurements Using Luminescent Coating 1," *Annual Review of Fluid Mechanics*, Vol. 33, No. 1, 2001, pp. 155–206. doi:10.1146/annurev.fluid.33.1.155

[34] Charbonnier, D., Ott, P., Jonsson, M., Cottier, F., and Köbke, T., "Experimental and Numerical Study of the Thermal Performance of a Film Cooled Turbine Platform," *ASME Turbo Expo 2009, Power for Land, Sea, and Air*, Vol. 3: Heat Transfer, American Soc. of Mechanical Engineers, Fairfield, NJ, 2009, pp. 1027–1038. doi:10.1115/GT2009-60306

[35] Johnson, B. E., and Hu, H., "Measurement Uncertainties Analysis in the Determination of Adiabatic Film Cooling Effectiveness by Using Pressure Sensitive Paint (PSP) Technique," *ASME 2014 4th Joint US-European Fluids Engineering Division Summer Meeting Collocated with the ASME 2014 12th International Conference on Nanochannels, Microchannels, and Minichannels*, American Society of Mechanical Engineers, Fairfield, NJ, 2014, Paper V01DT40A001. doi:10.1115/FEDSM2014-21230

[36] Melling, A., "Tracer Particles and Seeding for Particle Image Velocimetry," *Measurement Science and Technology*, Vol. 8, No. 12, 1997, pp. 1406–1416. doi:10.1088/0957-0233/8/12/005

J. P. Bons
Associate Editor